Journal of Inorganic Biochemistry

Photoactivation of *trans* platinum diamine complexes in aqueous solution and effect on reactivity towards nucleotides

Leticia Cubo[a,b], Ana M. Pizarro[b], Adoración Gómez Quiroga[a], Luca Salassa[b], Carmen Navarro-Ranninger[a,*] and Peter J. Sadler[b,*]

[a] *Departamento de Química Inorgánica, Universidad Autónoma de Madrid, 28049 Madrid, Spain*

[b] *Department of Chemistry, University of Warwick, Gibbet Hill Road, CV4 7AL, UK*

* Corresponding author. P.J.Sadler@warwick.ac.uk;

Tel: (+44) 024 76523818; Fax: (+44) 024 76523819

E-mail addresses: carmen.navarro@uam.es; P.J.Sadler@warwick.ac.uk

ABSTRACT

We show that UVA irradiation (365 nm) of the Pt^{IV} complex *trans,trans,trans*-[$Pt^{IV}Cl_2(OH)_2$(dimethylamine)(isopropylamine)], **1**, induces reduction to Pt^{II} photoproducts. For the mixed amine Pt^{II} complex, *trans*-[$Pt^{II}Cl_2$(isopropylamine)(methylamine)] (**2**), irradiation at 365 nm increases the rate and extent of hydrolysis, triggering the formation of diaqua species. Additionally, irradiation increases the extent of reaction of complex **2** with guanosine-5´-monophosphate (GMP) and affords mainly the bis-adduct, while reactions with adenosine-5´-monophosphate (AMP) and cytidine-5´-monophosphate (CMP) give rise only to mono-nucleotide adducts. Density Functional Theory calculations have been used to obtain insights into the electronic structure of complexes **1** and **2**, and their photophysical and photochemical properties. UVA-irradiation can contribute to enhanced cytotoxic effects of diamine platinum drugs with *trans* geometry.

Graphical Abstract

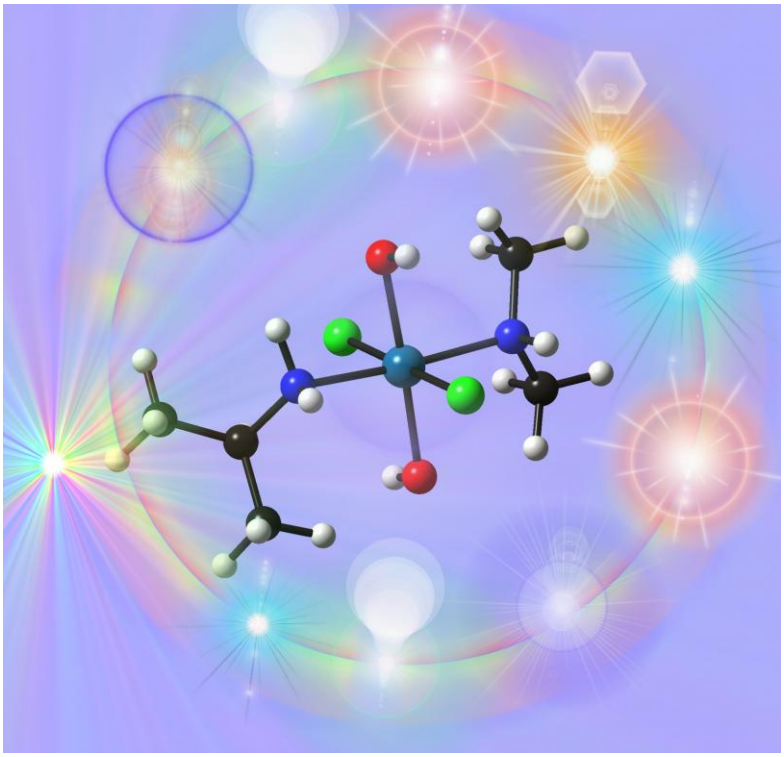

Irradiation at 365 nm induces activation of this *trans*-Pt^{IV} diamine dichlorido dihydroxido anticancer complex via reduction to reactive Pt^{II} species. Additionally, light promotes the second aquation of Pt^{II} dichlorido species and their interaction with guanosine monophosphate, leading mainly to bis-nucleotide adducts.

Keywords: Photoactivation, *trans*-platinum diamine, platinum anticancer complexes, DNA bases, NMR.

1. Introduction

In recent years there have been major advances in understanding the factors which control the binding of platinum anticancer drugs (such as cisplatin) to DNA and of the consequences of DNA binding, which ultimately lead to cell death [1, 2]. An important step in the activity of platinum anticancer complexes is activation through hydrolysis [3], which is often a necessary and rate-limiting step in their reactions with DNA and other biomolecules. Not only is there current interest in *cis* diam(m)ine platinum complexes, but also in *trans* diam(m)ine complexes which can also exhibit interesting activity [4-11], even though transplatin itself is inactive [12]. Our recent investigations of *trans* platinum complexes containing aliphatic amines, such as *trans*-[$PtCl_2$(^{15}N-ipa)(^{15}N-ma)], *trans*-[$PtCl_2$(^{15}N-dma)(^{15}N-ma)] and *trans*-[$PtCl_2$(^{15}N-dma)(^{15}N-ipa)] (ipa = isopropylamine, ma = methylamine, and dma = dimethylamine) by 2D [^{1}H,^{15}N] HMQC NMR spectroscopy suggest that the dichlorido (less reactive) species is the predominant form present in cancer cells under physiological conditions [13], despite the high cytotoxic activity exhibited by these complexes.

Photodynamic therapy (PDT) has attracted considerable attention for the treatment of a variety of cancers. The photochemistry of the platinum complexes is of particular interest since light can induce a wide range of electronic transitions [14]. Photoactivable Pt^{IV}-azide complexes represent a promising area for new drug development [15-17].

Photochemical studies on transplatin (*trans*-[$Pt^{II}Cl_2(NH_3)_2$]), cisplatin (*cis*-[$Pt^{II}Cl_2(NH_3)_2$]) and cisplatin-like complexes have shown that irradiation can induce substitution of chlorido ligands by solvent H_2O or DMSO [18-20]. UVA light promotes the loss of the second chlorido of transplatin and also promotes DNA binding and cytotoxicity

[21]. Here we investigate the possibility of using irradiation to activate the cytotoxic Pt^{IV} mixed diamine *trans* complex *trans*-[$Pt^{IV}Cl_2(OH)_2$(dimethylamine)(isopropylamine)], **1**, and the Pt^{II} analogue, *trans*-[$Pt^{II}Cl_2$(isopropylamine)(methylamine)], **2** (Figure 1) through photoreduction [22, 23] and photosubstitution. We report the effect of irradiation on the aqueous behaviour of complexes **1** and **2**. In addition, we have studied the influence of irradiation over time on reactions of complex **2** with the nucleotides guanosine-5´-monophosphate (GMP), adenosine-5´-monophosphate (AMP), and cytidine-5´-monophosphate (CMP) (Figure 1). The reactions have been monitored by NMR spectroscopy and the corresponding adducts in each case (Table 1) have been characterized by NMR and mass spectrometry.

2. Materials and Methods

Trans,trans,trans-[$PtCl_2(OH)_2$(dma)(ipa)], **1**, and *trans*-[$PtCl_2$(ipa)(ma)], **2**, were prepared using previously described procedures [24, 25]. Guanosine-5´-monophosphate (GMP), cytidine-5´-monophosphate (CMP) and 9-methyladenine (9MeA) were purchased from Sigma-Aldrich and adenosine-5´-monophosphate (AMP) from Acros Organic.

2.1. Sample preparation

Stock solutions of 2.5 mM platinum complex were prepared unless otherwise stated. Stock samples were diluted for MS and LC-MS as explained below. Reactions between platinum complexes and mononucleotides were performed at 1:2 molar ratios. The pH of the final solution in each experiment was adjusted in the range 6–7 with 0.1 M NaOH. All pH measurements were made at 298 K on a Martini MI150 pH meter equipped with a chloride-free semi-micro combination electrode (Thermo Fisher Scientific) calibrated with standard buffers (pH 4, 7 and 10, Aldrich).

2.2. Nuclear magnetic resonance (NMR) Spectroscopy

1D ^{1}H and 2D [^{1}H, ^{13}C] HSQC NMR spectra were recorded on a 500 MHz Bruker spectrometer using 5 mm tubes at 310 K. Solutions were prepared in 100 mM $NaClO_4$ and 90% H_2O / 10% D_2O with a final concentration [Pt] = 2.5 mM for ^{1}H and [^{1}H,^{13}C] HSQC, and 15 mM for ^{195}Pt NMR. ^{1}H, and ^{195}Pt NMR chemical shifts were internally referenced to TSP via 1,4-dioxane (3.76 ppm), and externally to K_2PtCl_6 (0 ppm), respectively. Water signals were suppressed using presaturation or Shaka methods [26].

2.3. Mass Spectrometry

MS characterization studies were carried out on an HCT-plus Bruker ion trap mass spectrometer. The final concentration used in these samples was 15 μM [Pt]. EsquireControl 5.2 software was used to analyse the MS spectra. Isotope modelling of the MS peaks was performed for all the assignments. Pt–9MeA adducts were characterized by ESI-MS on an API Q-START Pulsari Q-TOF mass spectrometer in the positive ion mode diluting the samples 50% with methanol. The final concentration was 50 μM [Pt].

2.4. Liquid Chromatography-Mass Spectrometry.

High performance liquid chromatography (HPLC) was carried out on an Agilent ChemStation 1100 Series instrument, with a DAD detector. Part of the outflow was routed to the Bruker HCT-plus ion trap MS. Hystar 3.0 software was used to analyse the LC-MS data. The final concentration used in the LC samples was 1 mM [Pt]. For all analytical separations, a RP C18 column (250 × 4.6 mm, 100 Å, 5 μm, Hichrom) was used, eluting with 5–30% acetonitrile gradients over varying time intervals with 0.1% trifluoroacetic acid as an ion-pairing agent and with UV detection at 275 nm.

2.5. Irradiation

The light source was a Luzchem LZC-ICH2 illuminator (photoreactor) oven using both Luzchem LZCUVA (Hitachi) and LZC-VIS (Sylvania cool white) lamps, with no other sources of light filtration. The photoreactor operated at 365 nm (λ_{max}) with temperature controller at 310 K and power level of 1.9 mW/cm^2. The power levels were monitored

using the appropriate probe window, calibrated with an OAI-306 UV power meter from Optical Associates, Inc.

2.6. Computational Details

All calculations were performed with the Gaussian 03 (G03) program [27] employing the DFT method and the PBE1PBE [28] functional. The LanL2DZ basis set [29] and effective core potential were used for the Pt atom and the 6-31G**+ basis set [30] was used for all other atoms. Geometry optimizations of **1** and **2** in the ground state (S_0) and lowest-lying triplet state (T_1) were performed in the gas phase and the nature of all stationary points was confirmed by normal mode analysis. For the T_1 geometries the UKS method with the unrestricted PBE1PBE functional was employed. The conductor-like polarizable continuum model method (CPCM) [31] with water as solvent was used to calculate the electronic structure and the excited states of **1** and **2** in solution. Thirty-two singlet excited states with the corresponding oscillator strengths were determined with a Time-dependent Density Functional Theory (TD-DFT) [32, 33] calculation. The electronic distribution and the localization of the singlet excited states were visualized using the electron density difference maps (EDDMs) [34-36]. GaussSum 1.05 was used for EDDMs calculations and GaussSum 2.2 for the electronic spectrum simulation (ν_{fwhm} = 4000 cm^{-1}) [37].

3. Results and Discussion

*3.1. Irradiation of trans,trans,trans-[$Pt^{IV}Cl_2(OH)_2(dma)(ipa)$] (**1**) in aqueous solution*

The thermal (dark, 310 K) and photo-induced (365 nm light) behaviour of complex **1** in water (2.5 mM, pH *ca.* 6) was monitored for 4 h using ^{1}H NMR spectroscopy. Characterization of the products after 4 h was carried out by LC-MS and ^{195}Pt NMR techniques.

The ^{1}H NMR spectrum of complex **1** in the dark over a period of 4 h (Figure 2A) showed no changes, indicating thermal stability. However, for the sample under irradiation (Figure 2B) several changes were observed. The doublet corresponding to the isopropylamine methyl groups (1.33 ppm) appears to split into two doublets, attributable to either isomerization and/or aquation of the Pt^{IV} complex as a result of the irradiation. Such effects have been documented previously for Pt^{IV} complexes containing halides and ammonia ligands, and have been used in synthesis [23, 38, 39]. Accordingly, it has been reported that irradiation of Pt^{IV} azide complexes gives rise to at least five additional Pt^{IV} light-induced photoproducts [16]. Irradiation gave rise to new ^{1}H resonances at 1.27 ppm corresponding to Pt^{II} species. This doublet is assignable to the methyl groups of the Pt^{II} counterpart [$PtCl_2$(dma)(ipa)]. This doublet appears to be composed of two overlapping doublets, likely to be geometrical isomers *cis* and *trans* [23]. Additionally when the sample was irradiated, proton resonances for Pt^{IV}–NH and Pt^{IV}–NH_2 groups (6.28 and 5.47 ppm, respectively) disappeared, and a new peak arose in the region of the Pt^{II}–NH_2 signals (broad signal at 4.04 ppm, not shown) which provided evidence for photoreduction of complex **1**. Several new peaks of low intensity were also observed in the high-field region

of the ^{1}H NMR spectrum of the irradiated sample, which can be assigned to photo-isomerisation and photo-substitution products formed upon irradiation.

In order to identify the nature of the photoproducts, the samples were analyzed by LC-MS. For the sample in the dark, elution produces only one peak at 7 min, and no differences were observed over 4 h (Figure S1A). However, when the sample was irradiated, the chromatogram showed two additional new peaks, eluting at 29 and 30 min (Figure S1B). The positive ion ESI-MS of the peak at 7 min showed a species at 426.96 *m/z* corresponding to $\{C_5H_{18}Cl_2N_2O_2Pt + Na\}^+$ assignable to complex **1** (Figure S2A). The ESI-MS data obtained for the two new peaks eluting at 29 and 30 min were alike (Figures S2B and S2C, respectively), showing a similar molecular ion at 376.07 and 376.02 *m/z*, respectively, both assignable to $\{C_5H_{17}ClN_2Opt + Na\}^+$, likely to be *cis* and *trans* isomers of reduced photoproducts of **1** [23].

The ^{195}Pt NMR spectrum of a sample of **1** (15 mM, pH *ca.* 6) was recorded before and after the irradiation. The Pt^{IV} complex **1** was the only species present in solution before the irradiation ($\delta(^{195}Pt)$ +798 ppm). After irradiation a signal at –2185 ppm appeared in the spectrum (Figure S3). ^{195}Pt NMR chemical shifts are highly dependent on the oxidation state of the metal, with Pt^{II} considerably more shielded than Pt^{IV} [40, 41]. The signal at –2185 ppm corresponds to a Pt^{II} species, supporting the photoreduction reaction [42]. However, the ^{195}Pt NMR spectrum failed to show any other Pt^{II} species, possibly because they do not accumulate in high enough concentration to be observed by ^{195}Pt NMR spectroscopy.

Comparison of the LC-MS and ^{195}Pt NMR results obtained for Pt^{IV} and its Pt^{II} analogue indicates that **1** undergoes reduction under UVA light, in agreement with previous results

obtained by ^{1}H NMR. The reduction mechanism of complex **1** in aqueous solution seems to be triggered, or at least promoted, by irradiation.

*3.2. Irradiation of trans-[Pt^{II}Cl$_2$(ipa)(ma)] (**2**) in aqueous solution*

We studied the effect of irradiation on the hydrolysis of **2**, *trans*-[PtCl$_2$(ipa)(ma)] by ^{1}H NMR. Figure 3A shows the progress of hydrolysis of complex **2** in the dark. Two sets of ^{1}H NMR signals at 1.27 and 1.31 ppm, assignable to isopropyl groups of the chloride (**2**) and monoaqua (**2A**) complexes, respectively. In the presence of light (Figure 3B), the same solution quickly gave rise also to a new set of peaks with a ^{1}H NMR chemical shift of 1.35 ppm, which is assignable to the diaqua species (**2AA**) [13]. Peaks corresponding to the diaqua species (**2AA**) are clearly dominant over the monoaqua species after 1.5 h irradiation (Figure 4). The diaqua species was detected only in the non-irradiated sample after 20 h [13].

Photolytic reactions of square-planar platinum(II) complexes in aqueous solutions include photoaquation and photoisomerizations [18, 20, 22]. For example, the photoaquation of *cis*- and *trans*-[Pt(NH$_3$)$_2$Cl$_2$], with the concomitant release of chlorido ligands, has been previously reported and the quantum yield values for the photolysis reaction of both isomers determined [20]. Additionally, irradiation of *trans*-[Pt(NH$_3$)$_2$Cl$_2$] induced further release of chloride in aqueous solution. The release of the second chloride from transplatin as a result of photoactivation may provide a mechanism for activation of the inactive *trans* complex [21].

*3.3. DFT and TD-DFT studies of photoactivation mechanisms for **1** and **2***

DFT and TD-DFT calculations have been successfully employed to obtain insights in the mechanism of photoactivation of several metal complexes [43-46]. Characterization of singlet and triplet states (in the case of diamagnetic d^6 metal complexes) can reveal fundamental information on such process. For this reason, the singlet ground state (S_0) and the lowest-lying triplet state (T_1) geometries were optimized for both **1** and **2** and thirty-two singlet states were calculated by TD-DFT from the S_0 geometries of the two complexes to characterize their UV-Vis properties. A comparison between the calculated and experimental UV-Vis spectra of **1** and **2** is reported in the Supporting Information (Figures S4–S6 and Tables S1–S4), together with the orbital composition of selected singlet transitions. Interestingly, such calculations highlight that all the UV-Vis singlet transitions of **1** and **2** in the 210–500 nm range involve the LUMO orbital (Figure 5), which is σ*-antibonding. The contribution of this orbital gives a strong dissociative character to such transitions, particularly towards the Pt–Cl bonds. This result is consistent with the labilization of the chlorido ligands upon light excitation. Furthermore, the lowest-lying triplet state (generally populated after the intersystem crossing promoted by the metal spin-orbit coupling occurs) is dissociative as well. The highest-SOMO, in fact, corresponds to the LUMO of the ground state (shown in Figure 5), resulting in a dissociative state. The lowest-lying triplet geometry of **1** is distorted and has elongated Pt–Cl bonds, consistent with the dissociation of one of these ligands (Table 2). In the case of **2** the elongation of Pt–Cl bonds upon triplet formation is limited, although there is a strong distortion of the Cl–Pt–Cl angle. As shown previously in the case of other photoactive Pt^{IV} derivatives, the dissociation of one or more chlorido ligands and the subsequent formation of hydroxo-species can lead to the reduction of the Pt centre via reductive photoelimination [47].

*3.4. Photoinduced reactivity of trans-[$Pt^{II}Cl_2$(ipa)(ma)] (**2**) with DNA model bases*

We studied the effect of irradiation on reactions of complex **2**, *trans*-[$PtCl_2$(ipa)(ma)], with the nucleotides: guanosine-5´-monophosphate (GMP), adenosine-5´-monophosphate (AMP) and cytidine-5´-monophosphate (CMP).

*3.4.1. Reactivity of trans-[$PtCl_2$(ipa)(ma)] (**2**) with GMP*

The photoinduced reaction between complex **2** and two mol equivalents of GMP was monitored by ^{1}H NMR by following the changes in the H8 peak of GMP (Figure 6), a resonance which is often useful for monitoring interactions of this nucleotide with metal complexes [48, 49]. The following GMP H8 peaks were assigned: 8.15 ppm, free nucleotide; 8.84 ppm for the mono-nucleotide adduct complex **3**, *trans*-[PtCl(GMP)(ipa)(ma)]$^+$; and 8.97 ppm for the bis-adduct *trans*-[$Pt(GMP)_2$(ipa)(ma)]$^{2+}$ complex **4**. The intensity of the H8-**4** signal (bis-adduct) in the photoinduced reaction was stronger than for the mono-nucleotide adduct after 4.5 h and also increased faster than for the non-irradiated sample (Figure 7). Monitoring the H8 chemical changes of the GMP ligand from the mono- and bis-nucleotide adducts *versus* pH suggests that the platination occurs at N7 of GMP since chemical shift changes associated with the pK_a of the N7 were not observed, i.e. no changes in the H8 chemical shift of platinated GMP in the pH range 2–4 (Figure S7) [50]. Similar results have been reported for complex **2** on reaction with 4 mol equivalents of GMP (10 mM $NaClO_4$, 310 K) under non-controlled lighting conditions [51].

The presence of mono- and bis-GMP adducts was confirmed by MS. The mass spectrum of the non-irradiated sample (Figure S8A) showed the mono-nucleotide species: $[PtCl(GMP)(ipa)(ma)]^+$ (**3**), assigned from the peak at *m/z* 684.12, $\{C_{14}H_{28}ClN_7O_8PPt\}^+$, and the sodium adduct at *m/z* 706.09, $\{C_{14}H_{27}ClN_7O_8PPt + Na\}^+$. Minor peaks were detected at *m/z* 665.16, $\{C_{14}H_{29}N_7O_9PPt\}^+$, assignable to the hydrolysed mono-nucleotide adduct $[Pt(H_2O)(GMP)(ipa)(ma)]^{2+}$ (**3A**) and *m/z* 1010.23, $\{C_{24}H_{41}N_{12}O_{16}P_2Pt\}^+$, and (paired with sodium ion) 1032.18, $\{C_{24}H_{40}N_{12}O_{16}P_2Pt + Na\}^+$, both assignable to the bis-nucleotide adduct $[Pt(GMP)_2(ipa)(ma)]^{2+}$ (**4**). In the MS of the irradiated sample, the signals for the bis-nucleotide adduct were significantly more intense (Figure S8B), in agreement with the NMR results. The predominance of the bis-GMP adduct signals over the mono-nucleotide adduct has been reported for complex **2** [51] and other similar *trans*-platinum(II) complexes, such as *trans*-$[PtCl_2(NH_3)(c\text{-}C_6H_{11}NH_2)]$ [52], under thermal conditions. However, in those cases, the reaction requires a significantly longer period of time (14 h for **2**, and *ca.* 24 h for the latter) to achieve a similar percentage of speciation. The use of irradiation appears to activate and enhance the formation of the bis-nucleotide adduct **4**. However, unlike the findings for transplatin, where the complex was totally consumed at the end of a 3 h-irradiation [21], most of complex **2** (*ca.* 75%) stays in the original dichlorido form. On the other hand, total conversion of transplatin into *trans*-$[Pt(NH_3)_2(GMP)_2]^{2+}$ under non-irradiating conditions has been reported to occur within five hours at 308 K when the Pt/nucleotide ratio was 0.5 [48].

*3.4.2. Reactivity of trans-$[PtCl_2(ipa)(ma)]$ (**2**) with AMP*

The effect of irradiation on the reaction of complex **2** with AMP was also investigated and monitored by NMR spectroscopy. The changes in the H8 and H2 ^{1}H NMR signals of AMP and its platinated adducts were followed over the first 4.5 hours. Two doublets were detected for both H8 and H2 with chemical shifts of 9.26 ppm (H8-**5**) and 9.15 ppm (H8-**5A**) for H8, and 8.40 (H2-**5**) and 8.38 (H2-**5A**) for H2, in both non-irradiated and the irradiated samples (Figure 8). These signals in the ^{1}H NMR spectra indicate the presence of two different AMP adducts. The ^{1}H NMR signals of both adducts were of higher intensity after 4.5 h in the dark than under irradiation (Figure S9 shows the species distribution curves over 4.5 h).

The Pt–AMP adducts were characterized by MS. No bis-adducts were detected in the reaction of **2** with AMP. Two different species were assigned in the MS spectra to the following mono-nucleotide adducts: $[PtCl(AMP)(ipa)(ma)]^{+}$ (**5**) to the peak at *m/z* 668.12 ($\{C_{14}H_{28}ClN_7O_7PPt\}^{+}$), and peak at *m/z* 690.10, $\{C_{14}H_{27}ClN_7O_7PPt + Na\}^{+}$ and $[Pt(OH)(AMP)(ipa)(ma)]^{+}$ (**5A**) to the peak at *m/z* 649.16, $\{C_{14}H_{29}N_7O_8PPt\}^{+}$ (Figure S10).

In order to complete the assignment of the peaks observed by NMR, the magnitudes of chemical shift differences for H8C8 and H2C2 between the free base and the metallated base in the 2D [^{1}H,^{13}C] NMR spectra were analysed, since this appears to be a useful diagnostic tool [53, 54] for assignment of the type of binding in metal-nucleotide adducts. The shift changes for the ^{13}C resonances were similar and small (up to *ca.* 3 ppm) for both mono-nucleotide adducts (Figure 9). The H8-adenine proton resonance, however, was low-field-shifted by up to *ca.* 0.7 ppm compared to free AMP for both complexes **5** and **5A**, while the H2 proton resonance was low-field-shifted by *ca.* 0.1 ppm compared to free AMP for both adducts. The greater shift changes in both species for proton H8 compared to H2

are attributed to *N7* (as opposed to *N1*) AMP-Pt coordination [54]. A NOESY spectrum of the sample after 4 h of reaction of **2** and 5´-AMP showed cross-peaks only between the H8 of the bound nucleotide and the isopropylamine and methylamine ligands in the platinum complex at 9.26 and 9.15 ppm, also suggesting coordination at *N7*. Interestingly, the two doublets, assigned to H8 in both mono-nucleotide adducts **5** and **5A** ($[PtCl(AMP)(ipa)(ma)]^+$ at 9.26 and $[Pt(OH)(AMP)(ipa)(ma)]^+$ at 9.15 ppm, respectively), coalescenced into one doublet upon lowering the pH with $HClO_4$ (Figure S11). On increasing the pH to give basic solutions, however, the intensity of the H8-signal corresponding to one of the mono-nucleotide adducts decreased with concomitant increase in intensity of the H8-signal of the other mono-nucleotide adduct, hence the assignment of the former signal to **5**, and the latter to **5A**. Additionally, treatment of the solution mixture with 0.15 M NaCl resulted in an increase in the intensity of the peaks assigned to **5**, although the anation was incomplete. Further addition of NaOH solution reversed the equilibrium towards **5A**.

LC-MS studies were carried out (mobile phase 0.1% TFA methanol/water, pH 2). Two different species were separated: AMP was detected as unreacted starting material at 348.06 *m/z*, $\{C_{10}H_{15}N_5O_7P\}^+$, and the mono-nucleotide adduct complex **5**, $[PtCl(AMP)(ipa)(ma)]^+$, at 668.09 *m/z*, $\{C_{14}H_{28}ClN_7O_7PPt\}^+$. Under acidic conditions the only mono-nucleotide adduct present was complex **5**, $[PtCl(AMP)(ipa)(ma)]^+$.

The assignation of species **5** and **5A** was confirmed by an experiment carried out with another adenine derivative, 9-methyladenine (9MeA). When complex **2** was reacted with 9MeA (Pt/nucleobase ratio 1:2, pH *ca.* 6.3, 24 h) three adducts were observed in the ^1H NMR spectrum after just one hour (Figure S12). The ESI-MS recorded after 24 h showed

two peaks at *m/z* 451.15 ($\{C_{10}H_{22}N_7OPt\}^+$) and 470.12 ($\{C_{10}H_{21}ClN_7Pt\}^+$), assignable to *trans*-[Pt(OH)(9MeA)(ipa)(ma)]$^+$ and *trans*-[PtCl(9MeA)(ipa)(ma)]$^+$, respectively. No bis-nucleotide adducts were detected. Analysis of the 2D [^{1}H,^{13}C] HMQC NMR spectra allowed assignment of the three adducts as [PtCl(*N7*-9MeA)(ipa)(ma)]$^+$ (**6**), [Pt(OH/OH$_2$)(*N7*-9MeA)(ipa)(ma)]$^{+/2+}$ (**6A**), and [PtCl(*N1*-9MeA)(ipa)(ma)]$^+$ (**7**) (Figure 10). The assignment is based on the extent of shift of the 2D [^{1}H,^{13}C] H8C8 and H2C2 signals of the platinated nucleobase when compared to those of the free nucleobase. *N7*-coordination produced more pronounced low-field shifts (by up to *ca.* 0.8 ppm) of H8 in *N7*-metallated adenine, while as little as *ca.* 0.2 ppm for H2. Conversely, *N1*-coordination produced low-field shifts by up to *ca.* 0.6 ppm for H2 in *N1*-metallated adenine, *versus* 0.1 ppm for H8. The ESI-MS under acidic conditions (0.5% TFA) showed only the mono-chlorido/mono-9MeA adduct, [PtCl(9MeA)(ipa)(ma)]$^+$, in agreement with the observations on the reaction of complex **2**, *trans*-[PtCl$_2$(ipa)(ma)], with AMP.

Similarly, Liu *et al.* have reported an analogous behaviour for the thermal reaction of *trans*-[PtCl$_2$(*E*-iminoether)$_2$] with one mol equivalent of GMP or AMP. *Trans*-[PtCl$_2$(*E*-iminoether)$_2$] appears to form two different mono-nucleotide adducts in aqueous solution at equilibrium (298 K), *trans*-[PtCl(*E*-iminoether)$_2$(nucleotide)]$^+$ and *trans*-[Pt(OH$_2$)(*E*-iminoether)$_2$(nucleotide)]$^{2+}$. The latter reversibly converts into the chlorido species at low pH and at high chloride concentration [55].

Interestingly, the proton resonances corresponding to H8 and H2 for the Pt–AMP adducts show doublet splitting whilst the Pt–GMP and Pt–9MeA complexes did not. This splitting effect may arise from hindered rotation about the Pt–N bond [56-58]. However, temperature-dependent NMR experiments failed to show coalescence up to 323 K. In

agreement with the observations of this work, Marzilli *et al.* have observed greater steric effects in $Pt^{II}(AMP)_2$ adducts in comparison to $Pt^{II}(GMP)_2$ adducts, as confirmed by the coalescence temperature [57]. Additionally, Lippert *et al.* have previously observed an H2 splitting phenomenon for *trans*-$[Pt(MeNH_2)_2$(1-MeT-*N3*)(9-MeA-*N1*)$]^+$ in D_2O. The authors attributed this to hindered rotation of the nucleobases about the Pt–N bonds. Most importantly, it appears that hindered rotation depends on the presence of methylamine ligands bound to Pt since the NH_3 analogue did not exhibit the same behaviour [59, 60].

*3.4.3. Reactivity of trans-[$PtCl_2$(ipa)(ma)] (**2**) with CMP*

Brabec and Leng showed that transplatin forms preferably GC interstrand crosslinks over GG adducts under competitive conditions [61]. The reaction of complex **2** with CMP in the dark and under irradiation at 365 nm was followed by ^{1}H NMR spectroscopy and ESI-MS. The ^{1}H NMR doublet corresponding to H6 of the cytidine mono-adducts was monitored over various irradiation times. Two new low-field-shifted doublets appeared and little difference was observed in the 1D ^{1}H NMR spectra of irradiated samples in comparison to those kept in the dark (Figures S13 and S14). Accordingly, the ESI-MS data showed comparable spectra after 4 h reaction under irradiation and thermal conditions (Figure S15), with the main species being complex **8**, $[PtCl(CMP)(ipa)(ma)]^+$, as a molecular ion at *m/z* 644.10 $\{C_{13}H_{28}ClN_5O_8PPt\}^+$ and *m/z* 666.07 $\{C_{13}H_{27}ClN_5O_8PPt + Na\}^+$. No bis-adducts were detected by MS. When the NMR sample was acidified to pH 2 only one Pt–CMP adduct remained (Figure S16). Increasing the pH to 11 did not have an effect on the intensity of the signals. Due to the similarities between this reaction and the reaction of complex **2** with AMP, we tentatively assign the two new adducts as the mono-

CMP/mono-chlorido adduct and mono-CMP/mono-aqua adduct, complexes **8** and **8A**, respectively. Additionally, Figure S16B confirms CMP preferential binding to the metal centre through *N3*, which represents the more basic site (pK_a 4.6) as compared to *N4* (pK_a 17) [50].

4. **Conclusions**

Irradiation with UVA light (365 nm) of complex **1**, *trans,trans,trans*-[$Pt^{IV}Cl_2(OH)_2$(dimethylamine)(isopropylamine)], in aqueous solution promotes reduction of platinum(IV) to platinum(II). When complex **2**, *trans*-[$PtCl_2$(ipa)(ma)], was irradiated in aqueous solution, the formation of bis-aqua species was facilitated. TD-DFT calculations suggested that all the UV-Vis singlet transitions of **1** and **2** in the 210–500 nm range involve the σ*-antibonding LUMO orbital, which has a strongly dissociative character (favouring Pt–Cl dissociation). The lowest-lying triplet state is dissociative as well. When an aqueous solution of **2** was irradiated in the presence of two mol equivalents GMP, formation of bis-adduct $[Pt(GMP)_2(ipa)(ma)]^{2+}$ was favoured; however, this was not the case for AMP nor CMP. When complex **2** reacted with AMP the mono-nucleotide adduct species $[PtCl(AMP)(ipa)(ma)]^{+}$, **5**, and $[Pt(OH)(AMP)(ipa)(ma)]^{+}$, **5A**, were detectable by NMR as the main Pt–AMP adducts in solution. Interestingly, when **2** was reacted with phosphate- and sugar-free nucleobase derivative 9MeA, a new *N1*-bound species was found. When complex **2** reacted with CMP, only mono-nucleotide adducts $[PtCl(CMP)(ipa)(ma)]^{+}$ (**8**) and $[Pt(CMP)(ipa)(ma)(OH/OH_2)]^{+/2+}$ (**8A**) could be observed and no bis-nucleotide adduct was detected. Our experiments suggest that irradiation at 365 nm can be used to activate *trans*-Pt^{IV} di-amine complexes and aid the formation of bis-nucleotide adducts with guanine derivatives, the preferred binding site for DNA-targeting platinum drugs.

Acknowledgements

We thank the Spanish Ministry of Science and Education (Grants SAF2006-03296 and SAF2009-09431), Medical Research Council (Grant G0701062 for AMP/PJS), Engineering and Physical Sciences Research Council (Grant G006792 for PJS), UAM (graduate student fellowship for LC), and EC (Marie Curie Intra European Fellowship 220281 PHOTORUACD within the 7th European Community Framework Programme for LS) for support. We also thank Dr Lijiang Song and Dr Adam Clarke (Warwick University) for assistance with mass spectrometry and NMR spectroscopy, respectively, and members of EC COST Action D39 for stimulating discussions.

References

[1] Y. Jung, S.J. Lippard, Direct Cellular Responses to Platinum-Induced DNA Damage, Chem. Rev. 107 (2007) 1387-1407.

[2] D. Wang, S.J. Lippard, Cellular processing of platinum anticancer drugs, Nat. Rev. Drug Discovery 4 (2005) 307-320.

[3] S.J. Berners-Price, T.G. Appleton, The chemistry of cisplatin in aqueous solution, Platinum-Based Drugs Cancer Ther. (2000) 3-35.

[4] N. Farrell, L.R. Kelland, J.D. Roberts, M. Van Beusichem, Activation of the trans geometry in platinum antitumor complexes: a survey of the cytotoxicity of trans complexes containing planar ligands in murine L1210 and human tumor panels and studies on their mechanism of action, Cancer Res. 52 (1992) 5065-5072.

[5] C. Manzotti, G. Pratesi, E. Menta, R.D. Domenico, E. Cavalletti, H.H. Fiebig, L.R. Kelland, N. Farrell, D. Polizzi, R. Supino, G. Pezzoni, F. Zunino, BBR 3464: a novel triplatinum complex, exhibiting a preclinical profile of antitumor efficacy different from cisplatin, Clin. Cancer Res. 6 (2000) 2626-2634.

[6] Y. Najajreh, E. Khazanov, S. Jawbry, Y. Ardeli-Tzaraf, J.M. Perez, J. Kasparkova, V. Brabec, Y. Barenholz, D. Gibson, Cationic Nonsymmetric Transplatinum Complexes with Piperidinopiperidine Ligands. Preparation, Characterization, in Vitro Cytotoxicity, in Vivo Toxicity, and Anticancer Efficacy Studies, J. Med. Chem. 49 (2006) 4665-4673.

[7] M. Coluccia, A. Nassi, F. Loseto, A. Boccarelli, M.A. Mariggio, D. Giordano, F.P. Intini, P. Caputo, G. Natile, A trans-platinum complex showing higher antitumor activity than the cis congeners, J. Med. Chem. 36 (1993) 510-512.

[8] E.I. Montero, S. Diaz, A.M. Gonzalez-Vadillo, J.M. Perez, C. Alonso, C. Navarro-Ranninger, Preparation and Characterization of Novel trans-[PtCl2(amine)(isopropylamine)] Compounds: Cytotoxic Activity and Apoptosis Induction in ras-Transformed Cells, J. Med. Chem. 42 (1999) 4264-4268.

[9] G. Natile, M. Coluccia, Current status of trans-platinum compounds in cancer therapy, Coord. Chem. Rev. 216-217 (2001) 383-410.

[10] G. Natile, M. Coluccia, in: A. Sigel, H. Sigel (Eds.), Met. Ions Biol. Syst., vol. 42, Marcel Dekker, Inc., New York, Basel, Hong Kong, 2004, pp. 209-250.

[11] U. Kalinowska-Lis, J. Ochocki, K. Matlawska-Wasowska, Trans geometry in platinum antitumor complexes, Coord. Chem. Rev. 252 (2008) 1328-1345.

[12] M.J. Cleare, J.D. Hoeschele, Antitumor activity of Group VIII transition metal complexes. I. Platinum(II) complexes, Bioinorganic Chemistry 2 (1973) 187-210.

[13] L. Cubo, D.S. Thomas, J. Zhang, A.G. Quiroga, C. Navarro-Ranninger, S.J. Berners-Price, [1H,15N] NMR studies of the aquation of cis-diamine platinum(II) complexes, Inorg. Chim. Acta 362 (2009) 1022-1026.

[14] P.J. Bednarski, F.S. Mackay, P.J. Sadler, Photoactivatable platinum complexes, Anti-Cancer Agents Med. Chem. 7 (2007) 75-93.

[15] P.J. Bednarski, R. Gruenert, M. Zielzki, A. Wellner, F.S. Mackay, P.J. Sadler, Light-Activated Destruction of Cancer Cell Nuclei by Platinum Diazide Complexes, Chem. Biol. 13 (2006) 61-67.

[16] F.S. Mackay, J.A. Woods, H. Moseley, J. Ferguson, A. Dawson, S. Parsons, P.J. Sadler, A photoactivated trans-diammine platinum complex as cytotoxic as cisplatin, Chem.--Eur. J. 12 (2006) 3155-3161.

[17] F.S. Mackay, J.A. Woods, P. Heringova, J. Kasparkova, A.M. Pizarro, S.A. Moggach, S. Parsons, V. Brabec, P.J. Sadler, A potent cytotoxic photoactivated platinum complex, Proc. Natl. Acad. Sci. U. S. A. 104 (2007) 20743-20748.

[18] M. Pujol, V. Girona, M. Trillas, X. Domenech, Kinetics of cisplatin photoaquation in aqueous solution, J. Chem. Res., Synop. (1991) 258-259.

[19] H.C. Fry, C. Deal, E. Barr, S.D. Cummings, Photoactivation of dichloro(ethylenediamine)platinum(II), J. Photochem. Photobiol., A 150 (2002) 37-40.

[20] J.R. Perumareddi, A.W. Adamson, Photochemistry of complex ions. V. Photochemistry of some square-planar platinum(II) complexes, J. Phys. Chem. 72 (1968) 414-420.

[21] P. Heringova, J. Woods, F.S. Mackay, J. Kasparkova, P.J. Sadler, V. Brabec, Transplatin Is Cytotoxic When Photoactivated: Enhanced Formation of DNA Cross-Links, J. Med. Chem. 49 (2006) 7792-7798.

[22] V. Balzani, V. Carassiti, Photochemistry of some square-planar and octahedral platinum complexes, J. Phys. Chem. 72 (1968) 383-388.

[23] V. Balzani, V. Carassiti, in: V. Balzani, V. Carassiti (Eds.), Photochemistry of Coordination Compounds, Academic Press Inc., London and New York, 1970, pp. 245-269.

[24] L. Cubo, A.G. Quiroga, J. Zhang, D.S. Thomas, A. Carnero, C. Navarro-Ranninger, S.J. Berners-Price, Influence of amine ligands on the aquation and cytotoxicity of trans-diamine platinum(ii) anticancer complexes, Dalton Trans. (2009) 3457-3466.

[25] J.M. Perez, L.R. Kelland, E.I. Montero, F.E. Boxall, M.A. Fuertes, C. Alonso, C. Navarro-Ranninger, Antitumor and cellular pharmacological properties of a novel platinum(IV) complex: trans-[PtCl(2)(OH)(2)(dimethylamine) (isopropylamine)], Mol. Pharmacol. 63 (2003) 933-944.

[26] T.-L. Hwang, A.J. Shaka, Water suppression that works. Excitation sculpting using arbitrary waveforms and pulsed field gradients, J. Magn. Reson. 112 (1995) 275-279.

[27] M.J. Frisch, GAUSSIAN 03 (Revision C.02), Gaussian, Inc., Wallingford, CT, 2004.

[28] J.P. Perdew, K. Burke, M. Ernzerhof, Generalized gradient approximation made simple, Phys. Rev. Lett. 77 (1996) 3865-3868.

[29] P.J. Hay, W.R. Wadt, Ab initio effective core potentials for molecular calculations. Potentials for the transition metal atoms scandium to mercury, J. Chem. Phys. 82 (1985) 270-283.

[30] A.D. McLean, G.S. Chandler, Contracted Gaussian basis sets for molecular calculations. I. Second row atoms, Z = 11-18, J. Chem. Phys. 72 (1980) 5639-5648.

[31] M. Cossi, N. Rega, G. Scalmani, V. Barone, Energies, structures, and electronic properties of molecules in solution with the C-PCM solvation model, J. Comput. Chem. 24 (2003) 669-681.

[32] M.E. Casida, C. Jamorski, K.C. Casida, D.R. Salahub, Molecular excitation energies to high-lying bound states from time-dependent density-functional response theory: characterization and correction of the time-dependent local density approximation ionization threshold, J. Chem. Phys. 108 (1998) 4439-4449.

[33] R.E. Stratmann, G.E. Scuseria, M.J. Frisch, An efficient implementation of time-dependent density-functional theory for the calculation of excitation energies of large molecules, J. Chem. Phys. 109 (1998) 8218-8224.

[34] M. Head-Gordon, A.M. Grana, D. Maurice, C.A. White, Analysis of Electronic Transitions as the Difference of Electron Attachment and Detachment Densities, J. Phys. Chem. 99 (1995) 14261-14270.

[35] W.R. Browne, N.M. O'Boyle, J.J. McGarvey, J.G. Vos, Elucidating excited state electronic structure and intercomponent interactions in multicomponent and supramolecular systems, Chem. Soc. Rev. 34 (2005) 641-663.

[36] L. Salassa, C. Garino, G. Salassa, C. Nervi, R. Gobetto, C. Lamberti, D. Gianolio, R. Bizzarri, P.J. Sadler, Ligand-selective photodissociation from [Ru(bpy)(4AP)4]2+: a spectroscopic and computational study, Inorg. Chem. 48 (2009) 1469-1481.

[37] N.M. O'Boyle, J.G. Vos, GaussSum, Dublin City University. Available at http://gausssum.sourceforge.net, 2005.

[38] R. Kuroda, S. Neidle, I.M. Ismail, P.J. Sadler, Crystal and molecular structure of three isomers of dichlorodiamminedihydroxoplatinum(IV): cis-trans isomerization on recrystallization from water, Inorg. Chem. 22 (1983) 3620-3624.

[39] C.F.J. Barnard, J.F. Vollano, P.A. Chaloner, S.Z. Dewa, Studies on the Oral Anticancer Drug JM-216: Synthesis and Characterization of Isomers and Related Complexes, Inorg. Chem. 35 (1996) 3280-3284.

[40] J.R.L. Priqueler, I.S. Butler, F.D. Rochon, An overview of 195Pt nuclear magnetic resonance spectroscopy, Appl. Spectrosc. Rev. 41 (2006) 185-226.

[41] B.M. Still, P.G.A. Kumar, J.R. Aldrich-Wright, W.S. Price, 195Pt NMR - theory and application, Chem. Soc. Rev. 36 (2007) 665-686.

[42] P.S. Pregosin, Platinum-195 nuclear magnetic resonance, Coord. Chem. Rev. 44 (1982) 247-291.

[43] A. Vlcek, S. Zalis, Modeling of charge-transfer transitions and excited states in d6 transition metal complexes by DFT techniques, Coord. Chem. Rev. 251 (2007) 258-287.

[44] L. Salassa, C. Garino, G. Salassa, R. Gobetto, C. Nervi, Mechanism of ligand photodissociation in photoactivable [Ru(bpy)2L2]2+ complexes: a density functional theory study, J. Am. Chem. Soc. 130 (2008) 9590-9597.

[45] L. Salassa, H.I.A. Phillips, P.J. Sadler, Decomposition pathways for the photoactivated anticancer complex cis,trans,cis-[Pt(N3)2(OH)2(NH3)2]: insights from DFT calculations, Phys. Chem. Chem. Phys. 11 (2009) 10311-10316.

[46] S. Betanzos-Lara, L. Salassa, A. Habtemariam, P.J. Sadler, Photocontrolled nucleobase binding to an organometallic RuII arene complex, Chem. Commun. (2009) 6622-6624.

[47] H.I.A. Phillips, L. Ronconi, P.J. Sadler, Photoinduced reactions of cis,trans,cis-[PtIV(N3)2(OH)2(NH3)2] with 1-methylimidazole, Chem.--Eur. J. 15 (2009) 1588-1596.

[48] A.T.M. Marcelis, C.G. Van Kralingen, J. Reedijk, The interactions of cis- and trans-diammineplatinum compounds with 5'-guanosine monophosphate and 5'-deoxyguanosine monophosphate. A proton NMR investigation, J. Inorg. Biochem. 13 (1980) 213-222.

[49] M.I. Djuran, S.U. Milinkovic, Z.D. Bugarcic, 1H NMR investigation of competitive binding of sulfur-containing peptides and guanosine 5'-monophosphate to a monofunctional platinum(II) complex, J. Coord. Chem. 44 (1998) 289-297.

[50] B. Lippert, in: K.D. Karlin (Ed.), Progress in Inorganic Chemistry, vol. 54, John Wiley & Sons, Inc., Hoboken, New Jersey, 2005, pp. 385-447.

[51] E. Pantoja, A. Alvarez-Valdes, J.M. Perez, C. Navarro-Ranninger, J. Reedijk, Synthesis and characterization of new cis-[PtCl2(isopropylamine)(amine')] compounds: cytotoxic activity and reactions with 5'-GMP compared with their trans-platinum isomers, Inorg. Chim. Acta 339 (2002) 525-531.

[52] S.J. Barton, K.J. Barnham, U. Frey, A. Habtemariam, R.E. Sue, P.J. Sadler, [1H,15N] NMR kinetic studies of reactions of cis- and trans-[PtCl2(15NH3)(c-C6H1115NH2)] with guanosine 5'-monophosphate, Aust. J. Chem. 52 (1999) 173-177.

[53] C.G. Barry, C.S. Day, U. Bierbach, Duplex-Promoted Platination of Adenine-N3 in the Minor Groove of DNA: Challenging a Longstanding Bioinorganic Paradigm, J. Am. Chem. Soc. 127 (2005) 1160-1169.

[54] M.S. Ali, S.R. Ali Khan, H. Ojima, I.Y. Guzman, K.H. Whitmire, Z.H. Siddik, A.R. Khokhar, Model platinum nucleobase and nucleoside complexes and antitumor activity: X-ray crystal structure of [PtIV(trans-1R,2R-diaminocyclohexane)trans(acetate)2(9-ethylguanine)Cl]NO3.H2O, J. Inorg. Biochem. 99 (2005) 795-804.

[55] Y. Liu, M.F. Sivo, G. Natile, E. Sletten, Antitumor trans platinum adducts of GMP and AMP, Met.-Based Drugs 7 (2000) 169-176.

[56] U. Bierbach, N. Farrell, Modulation of Nucleotide Binding of trans Platinum(II) Complexes by Planar Ligands. A Combined Proton NMR and Molecular Mechanics Study, Inorg. Chem. 36 (1997) 3657-3665.

[57] M.D. Reily, L.G. Marzilli, Anti-Cancer platinum drug adducts with AMP: novel direct proton and platinum-195 and NMR evidence for slowly interconverting "head-to-tail" rotamers. Potential role of amine ligand bulk and NH groups in guanine selectivity and anti-cancer activity, J. Am. Chem. Soc. 108 (1986) 6785-6793.

[58] A. Anzellotti, S. Stefan, D. Gibson, N. Farrell, Donor atom preferences in substitution reactions of trans-platinum mononucleobase compounds: Implications for DNA-protein selectivity, Inorg. Chim. Acta 359 (2006) 3014-3019.

[59] K.S. Schmidt, J. Reedijk, K. Weisz, E.M.B. Janke, J.E. Sponer, J. Sponer, B. Lippert, Loss of Hoogsteen Pairing Ability upon N1 Adenine Platinum Binding, Inorg. Chem. 41 (2002) 2855-2863.

[60] O. Krizanovic, M. Sabat, R. Beyerle-Pfnuer, B. Lippert, Metal-modified nucleobase pairs: mixed adenine, thymine complexes of trans-a2platinum(II) (a = ammonia, methylamine) with Watson-Crick and Hoogsteen orientations of the bases, J. Am. Chem. Soc. 115 (1993) 5538-5548.

[61] V. Brabec, M. Leng, DNA interstrand cross-links of trans-diamminedichloroplatinum(II) are preferentially formed between guanine and complementary cytosine residues, Proc. Natl. Acad. Sci. U. S. A. 90 (1993) 5345-5349.

Table 1. Numbering scheme for Pt^{II} adducts of general formula *trans*-$[PtL_1L_2(ipa)(ma)]^{n+}$.

Complex	Ligand	
	L_1	L_2
2	Cl	Cl
2A	Cl	H_2O
2AA	H_2O	H_2O
3	GMP	Cl
3A	GMP	H_2O
4	GMP	GMP
5	AMP	Cl
5A	AMP	OH
6	N7-9MeA	Cl
6A	N7-9MeA	OH/OH_2
7	N1-9MeA	Cl
8	CMP	Cl
8A	CMP	OH/OH_2

Table 2. Selected calculated bond distances (Å) and angles (deg) for complexes **1** and **2**.

	Ground-State Geometry		**Lowest-Lying Triplet Geometry**	
	1	**2**	**1**	**2**
Pt–N(ma)	2.093	2.056	2.125	2.122
Pt–N(ipa)	2.062	2.056	2.114	2.111
Pt–O	2.028	-	1.933	-
Pt–O	2.021	-	1.932	-
Pt–Cl	2.363	2.348	2.664	2.486
Pt–Cl	2.357	2.350	2.645	2.487
N–Pt–N	174.2	179.1	175.8	178.9
O–Pt–O	177.3	-	176.7	-
Cl–Pt–Cl	179.8	178.9	174.1	116.9

Figure captions.

Figure 1. Structure of the platinum complexes and nucleotides studied in this work.

Figure 2. High-field region of the ^{1}H NMR spectra of complex **1**, *trans,trans,trans*-[$Pt^{IV}Cl_2(OH)_2$(dimethylamine)(isopropylamine)], in aqueous solution over time: (A) in the dark, and (B) under irradiation. The doublet corresponds to the CH_3-isopropylamine (above) and the broad signals (below) to the NH_2 and NH groups.

Figure 3. ^{1}H NMR spectra of complex **2**, *trans*-[$PtCl_2$(ipa)(ma)] in aqueous solution over time at 310 K: (A) in the dark, and (B) under irradiation. Labels: dichlorido (**2**), monoaqua (**2A**), diaqua (**2AA**).

Figure 4. Time dependence of the aquation of complex **1**, *trans*-[$PtCl_2$(ipa)(ma)]: (A) in the dark, (B) under irradiation. Labels: ◆, dichlorido (**2**), ■, monoaqua (**2A**), ▲, diaqua (**2AA**) and **–**, other species (**i**).

Figure 5. Selected orbitals (isovalue 0.02) for complex **1** and **2** for the singlet ground-state optimized geometry.

Figure 6. Progress of the reaction between complex **2** with GMP as monitored by ^{1}H NMR spectroscopy, showing changes in the H8 region: (A) in the dark, (B) under irradiation. Labels: H8, GMP free; **3**, [PtCl(GMP)(ipa)(ma)]$^{+}$; and **4**, [$Pt(GMP)_2$(ipa)(ma)]$^{2+}$. H8-GMP free chemical shift changes to higher field in the irradiated sample (B) indicates monophosphate group protonation (pK_a ~6.2) [ref. 50], since the pH of the sample shifted from 6.5 and 6.0 after the photoinduction reaction.

Figure 7. Kinetic profiles of complex **2** reactivity with GMP, (A) in the dark and (B) under irradiation. Labels: ■, GMP free; ●, complex **3**; ▲, complex **4**. The concentration of the bis-adduct complex **4** has been calculated taking into account the different stoichiometry.

Figure 8. Progress of the reaction between **2** and AMP as monitored by ^{1}H NMR (low field), (A) in the dark, (B) under irradiation. Labels: **H8** and **H2**, AMP free; **5**, [PtCl(AMP)(ipa)(ma)]$^{+}$; **5A**, [Pt(OH)(AMP)(ipa)(ma)]$^{+}$.

Figure 9. 2D [^{1}H, ^{13}C] HMQC NMR spectra from the reaction of AMP with complex **2** after 4.5 h, showing signals in the H8/C8 and H2/C2 regions. Labels: **5**, [PtCl(AMP)(ipa)(ma)]$^{+}$; **5A**, [Pt(OH)AMP(ipa)(ma)]$^{+}$; H8/C8 and H2/C2, AMP free.

Figure 10. 2D [^{1}H,^{13}C] HMQC NMR after 4 h of the reaction of complex **2** with 9MeA. Labels: **6**, *trans*-[PtCl(ipa)(ma)(*N7*-9MeA)]$^{+}$; **6A**, *trans*-[Pt(ipa)(ma)(*N7*-9MeA)(OH/OH$_2$)]$^{+/2+}$; **7**, *trans*-[PtCl(ipa)(ma)(*N1*-9MeA)]$^{+}$; and **H2/2** and **H8/C8**, 9MeA free.

Figure 1

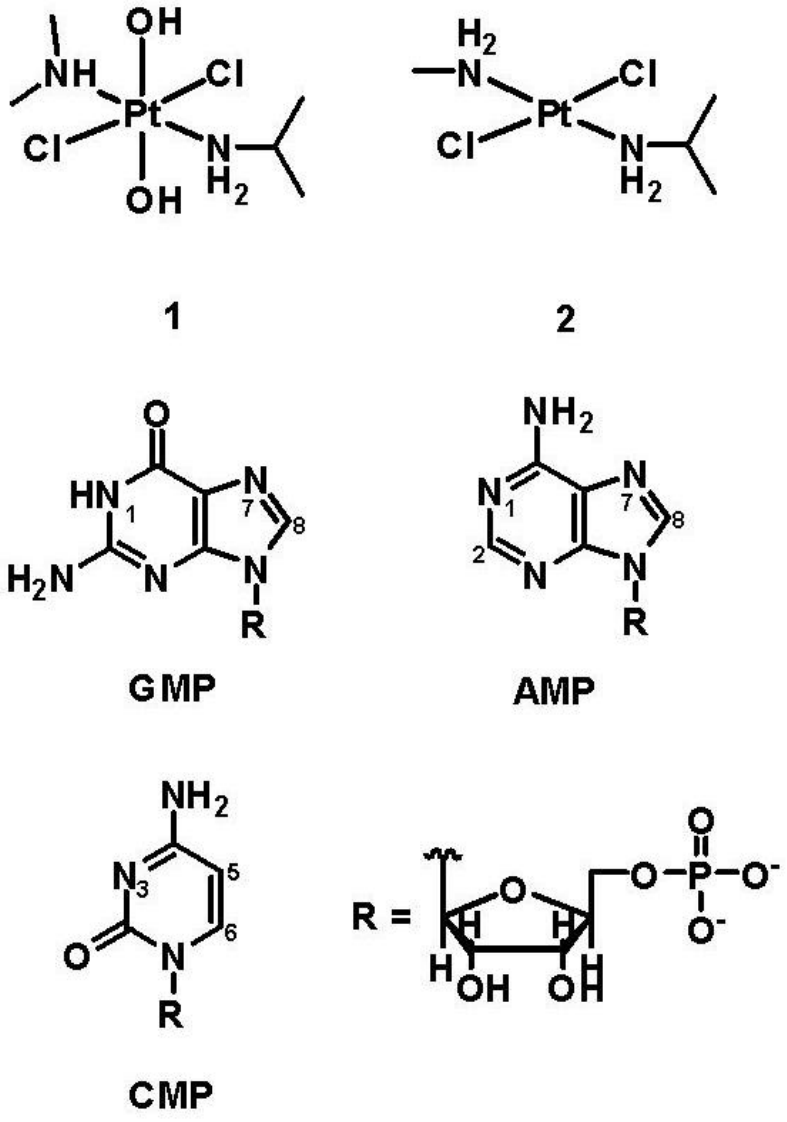
OH
NH
Cl
Pt
Cl
N
H2
OH
1
H2
N
Cl
Pt
Cl
N
H2
2
O
HN
1
N
7
8
H2N
N
N
R
GMP
NH2
N
1
N
7
8
2
N
N
R
AMP
NH2
N3
5
O
6
N
R
CMP
R =
O
O
P
O-
O-
O
H
H
H
OH
OH
H

Figure 2

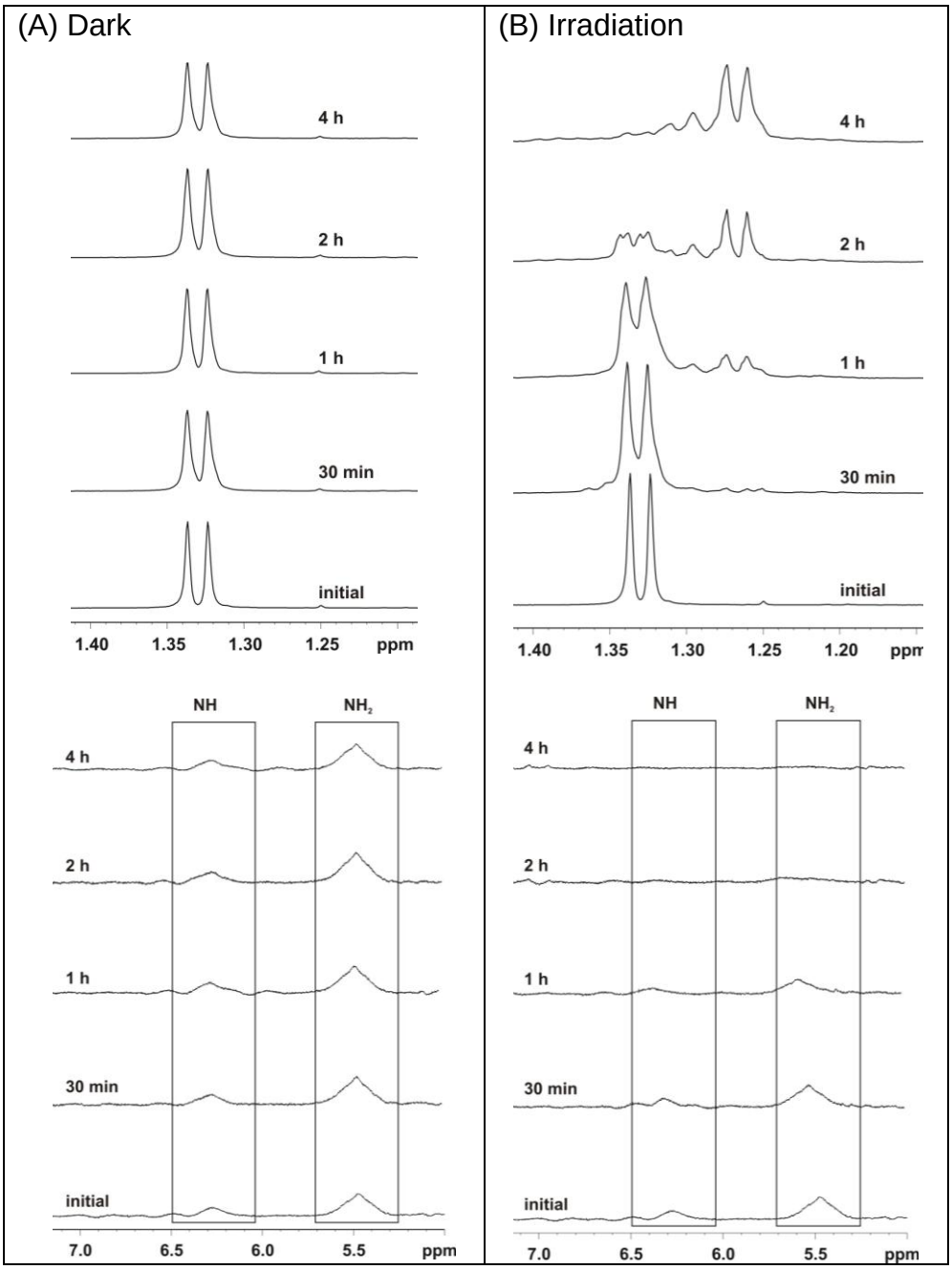
(A) Dark
(B) Irradiation
4 h
2 h
1 h
30 min
initial
1.40
1.35
1.30
1.25
1.20
ppm
NH
NH2
7.0
6.5
6.0
5.5

Figure 3

(A) Dark

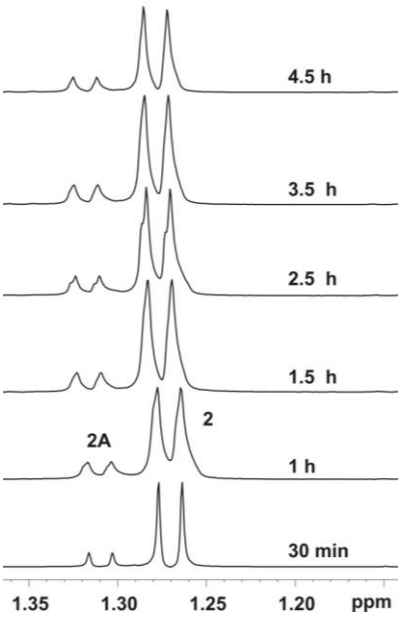

(B) Irradiation

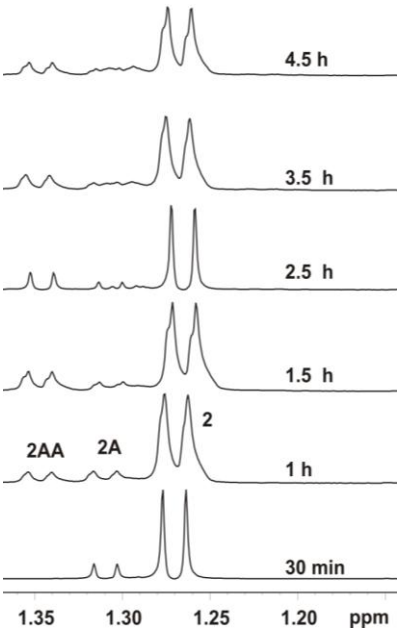

Figure 4

(A) Dark

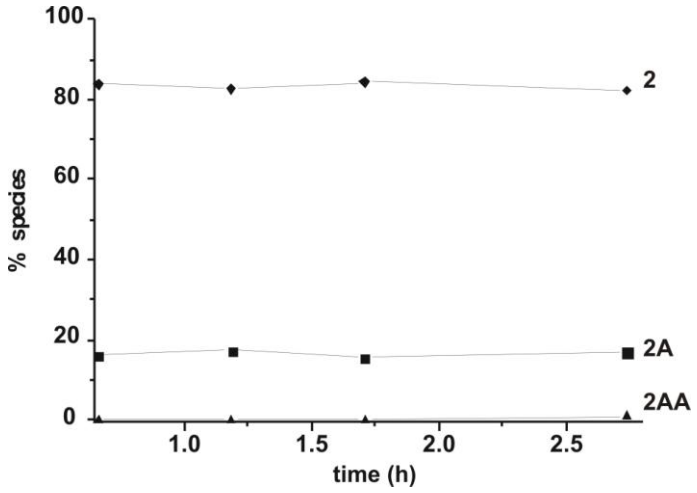

(B) Irradiation

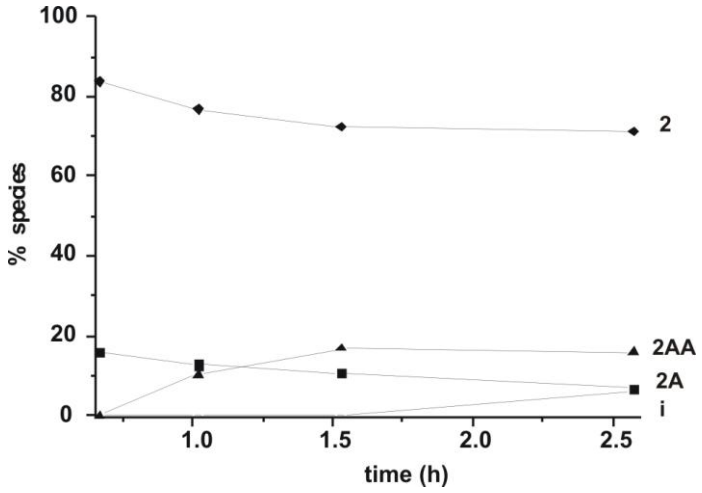

Figure 5

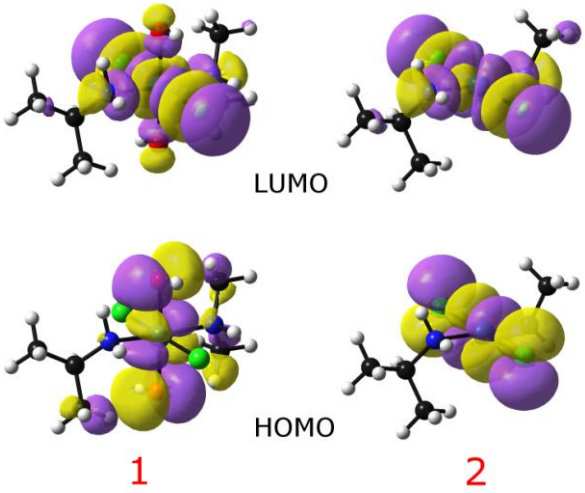

Figure 6
(A) Dark

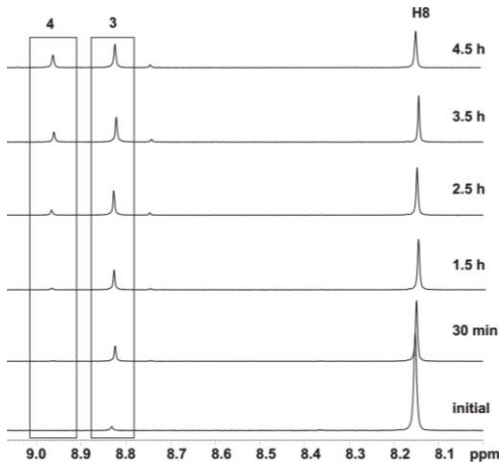

(B) Irradiation

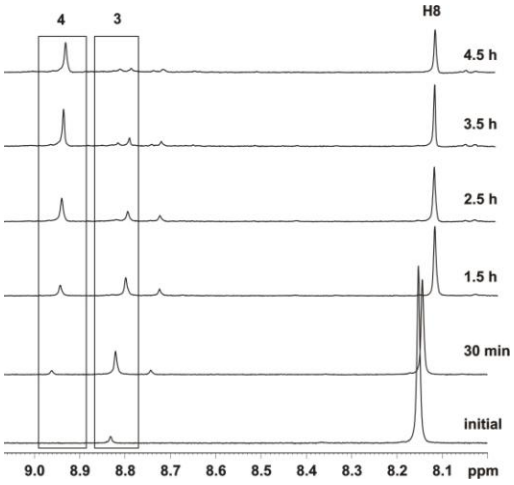

Figure 7

(A) Dark

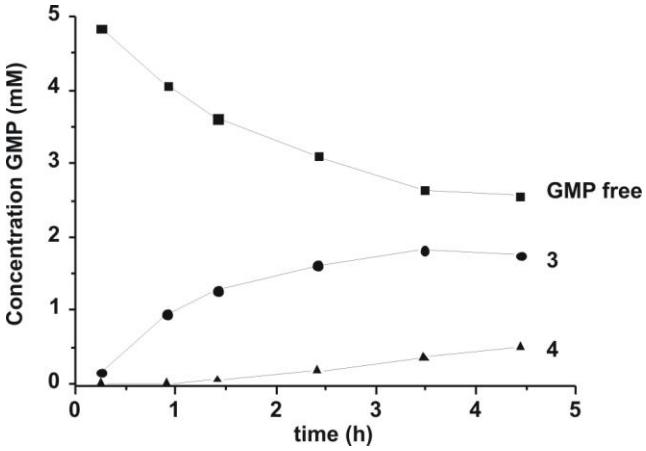

(B) Irradiation

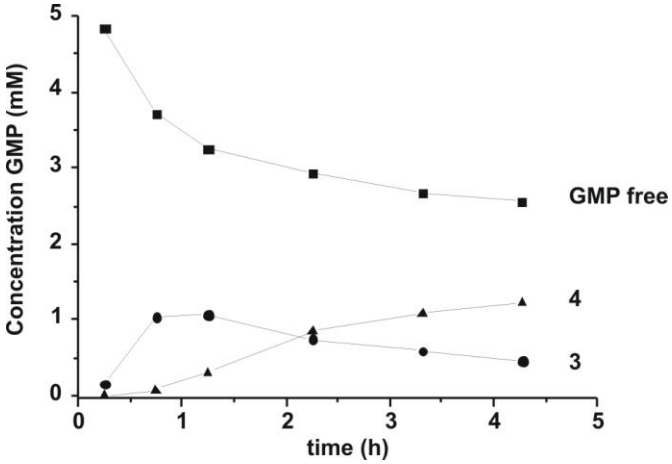

Figure 8

(A) Dark

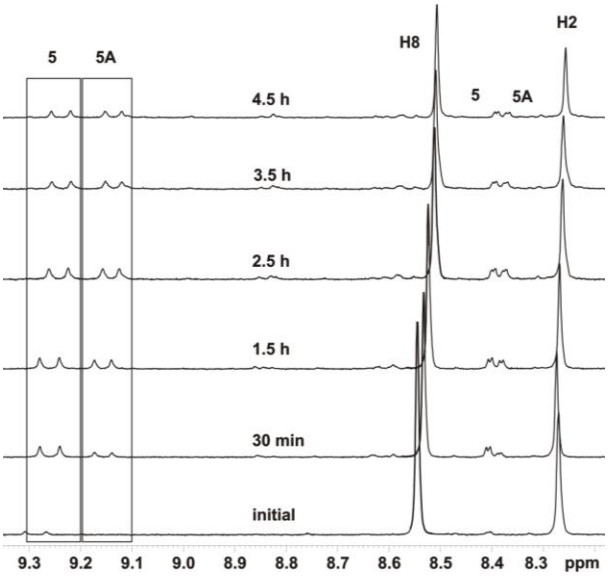

(B) Irradiation

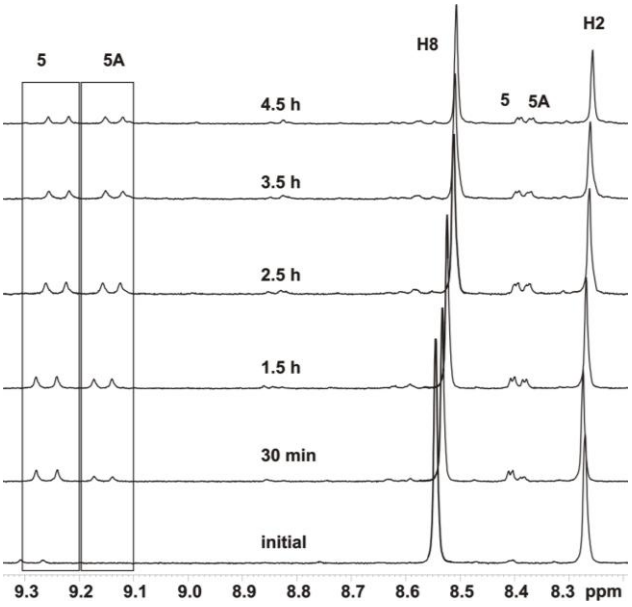

Figure 9

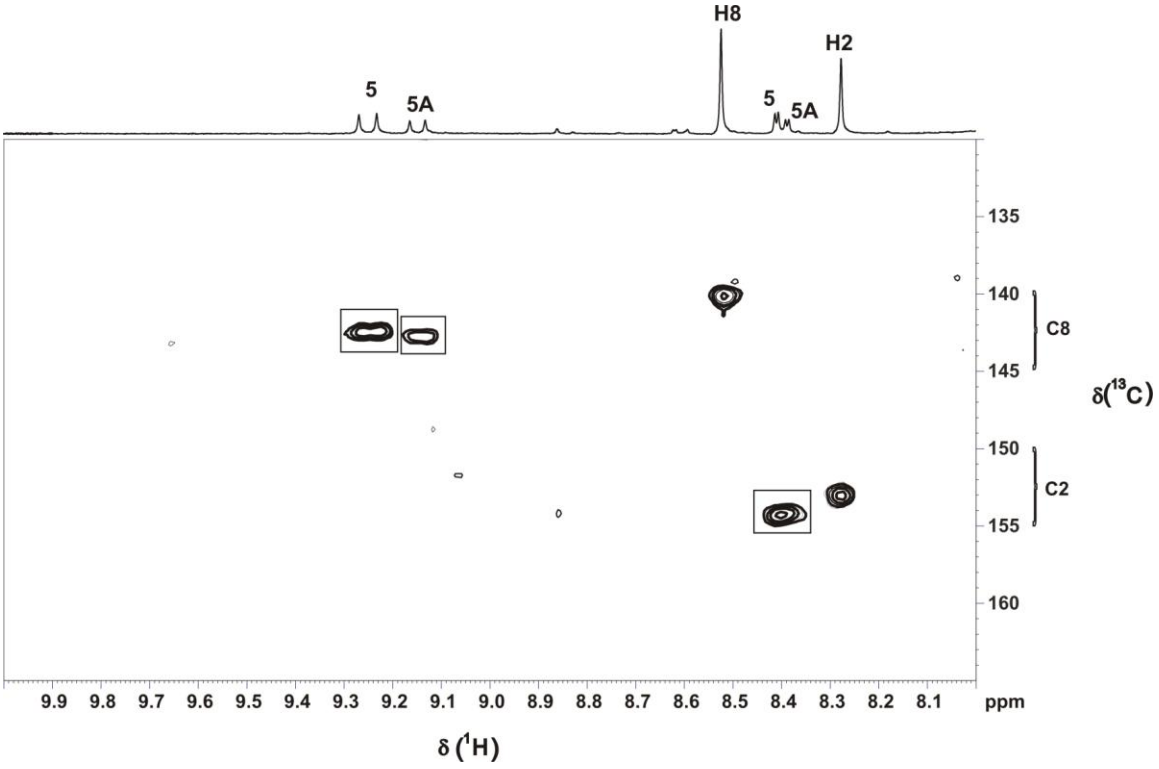
H8
H2
5
5A
5
5A
135
140
145
150
155
160
C8
C2
δ(13C)
9.9 9.8 9.7 9.6 9.5 9.4 9.3 9.2 9.1 9.0 8.9 8.8 8.7 8.6 8.5 8.4 8.3 8.2 8.1
ppm
δ (1H)

Figure 10

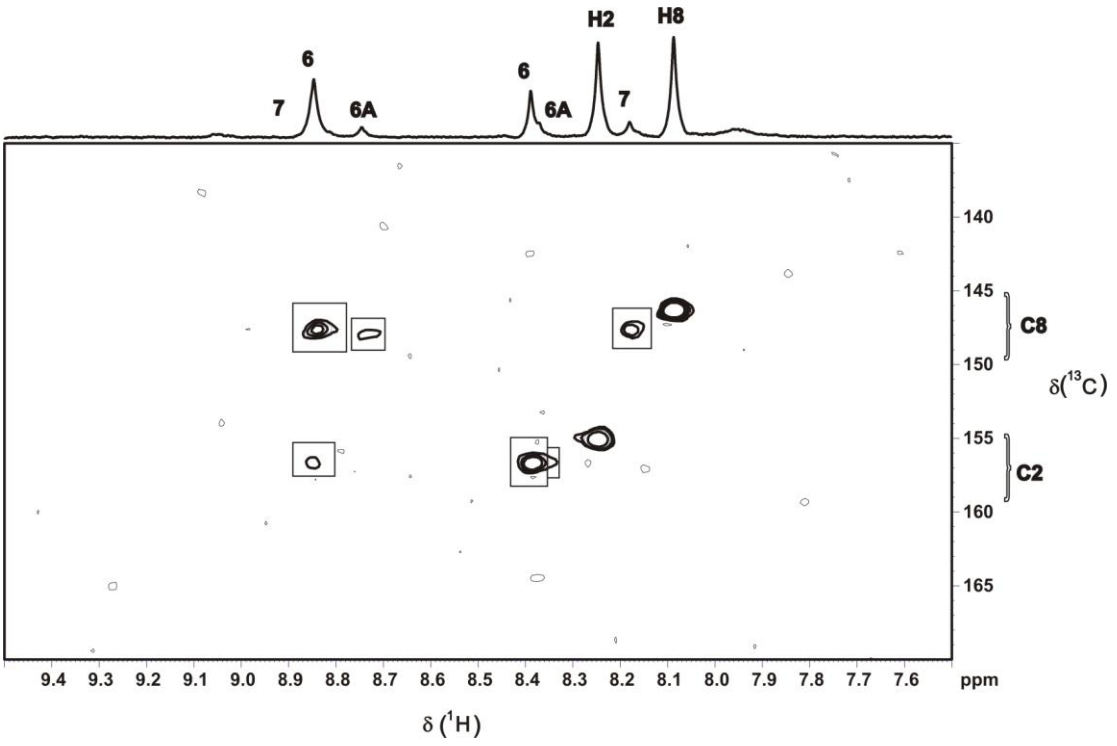
H2
H8
6
7
6A
6
6A
7
140
145
150
155
160
165
C8
C2
δ(13C)
9.4 9.3 9.2 9.1 9.0 8.9 8.8 8.7 8.6 8.5 8.4 8.3 8.2 8.1 8.0 7.9 7.8 7.7 7.6
ppm
δ (1H)